

---

# Parametric Mapping of Cerebral Blood Flow Deficits in Alzheimer's Disease: A SPECT Study Using HMPAO and Image Standardization Technique

Muhammad Babar Imran, Ryuta Kawashima, Shuichi Awata, Kazunori Sato, Shigeo Kinomura, Shuichi Ono, Seiro Yoshioka, Mitsumoto Sato and Hiroshi Fukuda

*Department of Nuclear Medicine and Radiology, Aoba Brain Research Imaging Center, Institute of Development, Aging and Cancer, Tohoku University, Sendai; and Department of Psychiatry, Tohoku University Hospital, Sendai, Japan*

---

This study assessed the accuracy and reliability of Automated Image Registration (AIR) for standardization of brain SPECT images of patients with Alzheimer's disease (AD). Standardized cerebral blood flow (CBF) images of patients with AD and control subjects were then used for group comparison and covariance analyses. **Methods:** Thirteen patients with AD at an early stage (age  $69.8 \pm 7.1$  y, Clinical Dementia Rating Score 0.5–1.0, Mini-Mental State Examination score 19–23) and 20 age-matched normal subjects (age  $69.5 \pm 8.3$  y) participated in this study.  $^{99m}\text{Tc}$ -hexamethyl propylenamine oxime (HMPAO) brain SPECT and CT scans were acquired for each subject. SPECT images were transformed to a standard size and shape with the help of AIR. Accuracy of AIR for spatial normalization was evaluated by an index calculated on SPECT images. Anatomical variability of standardized target images was evaluated by measurements on corresponding CT scans, spatially normalized using transformations established by the SPECT images. Re-aligned brain SPECT images of patients and controls were used for group comparison with the help of statistical parameter mapping. Significant differences were displayed on the respective voxel to generate three-dimensional Z maps. CT scans of individual subjects were evaluated by a computer program for brain atrophy. Voxel-based covariance analysis was performed on standardized images with ages and atrophy indices as independent variables. **Results:** Inaccuracy assessed by functional data was 2.3%. The maximum anatomical variability was 4.9 mm after standardization. Z maps showed significantly decreased regional CBF (rCBF) in the frontal, parietal and temporal regions in the patient group ( $P < 0.001$ ). Covariance analysis revealed that the effects of aging on rCBF were more pronounced compared with atrophy, especially in intact cortical areas at an early stage of AD. Decrease in rCBF was partly due to senility and atrophy, however these two factors cannot explain all the deficits. **Conclusion:** AIR can transform SPECT images of AD patients with acceptable accuracy without any need for corresponding structural images. The frontal regions of the brain, in addition to parietal and temporal lobes, may show reduced

CBF in patients with AD even at an early stage of dementia. The reduced rCBF in the cortical regions cannot be explained entirely by advanced atrophy and fast aging process.

**Key Words:**  $^{99m}\text{Tc}$ -hexamethyl propylenamine oxime SPECT; automated image registration; image standardization; Alzheimer's disease

**J Nucl Med 1999; 40:244–249**

---

**S**PECT is widely available and offers a sensitive diagnostic and research tool for the assessment of regional cerebral blood flow (rCBF) in Alzheimer's disease (AD). Although the predominant rCBF pattern observed with high posterior probability is one of bilateral parietotemporal abnormality (1), other patterns of rCBF deficits have also been reported in patients suffering from AD (2,3). Most of the previously reported studies have been retrospective, with patient selection based on the diagnosis established at the time of scintigraphic evaluation. Added to this, the subjective evaluation used in these cases for comparison with controls limited the sensitivity of the rating procedures. The effect of atrophy on CBF pattern has not been evaluated objectively or correlated for age in AD subjects. Moreover, evaluation of individual CBF images and intersubject comparison introduce error due to individual variance.

To address these issues, image standardization is used. Standardized images can be used for image averaging to improve signal-to-noise ratio. This will also take into account individual variance, making evaluation more accurate. Voxel-based covariance analyses and comparison of population samples by arithmetic and statistical calculations become possible. Any deviation from the normal pattern can be recognized and mapped out on the standard template with greater precision and accuracy.

Standardization of SPECT images has been tried by various techniques, including manual superimposition and derivation of transformation matrices (4,5). These vary in accuracy depending on the amount of information used in

---

Received Feb. 3, 1998; accepted Jun. 29, 1998.

For correspondence or reprints contact: Muhammad Babar Imran, MBBS, Department of Nuclear Medicine and Radiology, Division of Brain Sciences, Institute of Development, Aging and Cancer, Tohoku University, 4-1 Seiryomachi, Aoba-ku, Sendai, 980-8575 Japan.

computing the transformation matrices. Automated Image Registration (AIR, version 3) is a program recently developed by Woods et al. (6–8) that standardizes any brain image with respect to another specified reference image using linear and nonlinear models. Computation of registration parameters is based on functional data only. Because the program is noninteractive and is fully automated, the results of AIR are consistent and reproducible. The program has been validated for various types of registrations, including intersubject transformation of SPECT images of normal subjects (9–11). This software, however, has not been validated for CBF images of AD patients who have significantly advanced atrophy compared with normal subjects.

In this prospective study, we used AIR to standardize the size and shape of individual brain SPECT images of AD patients at an early stage and of age-matched healthy subjects after its validation for AD patients. Arithmetic and statistical calculations were performed on voxel values of individual images, and these were used to generate three-dimensional group mean images for further analyses. Effects of atrophy and age of individual subjects were evaluated by covariance analysis.

## MATERIALS AND METHODS

### Subjects

All procedures were approved by the Ethics Committee for Clinical Research of Tohoku University. A total of 13 AD patients (6 men, 7 women; age  $69.8 \pm 7.1$  y; Mini-Mental State Examination score 19–23; Clinical Dementia Rating Scale score 0.5–1.0) and 20 age-matched healthy subjects (8 men and 12 women; age  $69.5 \pm 8.3$  y) participated in the study. Written informed consent was obtained in all cases according to the Declaration of Human Rights of Helsinki 1975. All subjects were right-handed as assessed by the H.N. Handedness Inventory.

None of the control subjects had a history of any psychiatric disorder including drug abuse. Their past medical histories and physical examinations did not reveal any sign or symptom that could affect CBF studies. CT scans taken immediately after SPECT scanning were rated normal by radiologists.

Patients were diagnosed as probable AD according to criteria of the *Diagnostic and Statistical Manual of Mental Disorders*, Fourth Edition, and the National Institute of Neurological Disorders and Stroke and Alzheimer's Disease and Related Disorders Association (NINDS-ADRDA) by experienced psychiatrists. SPECT scans of AD subjects were obtained immediately after the diagnosis. In this study, we included only those subjects whose diagnoses remained the same after 1 y of follow-up. This was done to avoid inclusion of falsely diagnosed AD patients.

### Image Acquisition and Processing

Hexamethyl propylenamine oxime (HMPAO) was labeled with  $^{99m}\text{Tc}$  on site shortly before administration. The dose was approximately 1036 MBq (28 mCi). The radiopharmaceutical was injected in an antecubital vein while the subjects lay in supine positions with eyes closed in a secluded examination room. SPECT was performed 10 min after the injection. A SPECT scanner (SPECT-2000H; Hitachi Medico Corp., Tokyo, Japan) (12), incorporating a four-head rotating camera with an in-plane and axial resolution of 8 mm full width at half maximum (FWHM) fitted with low-energy,

high-resolution collimators, was used for scanning. Image reconstruction was performed by filtered backprojection using a Butterworth filter (dimension 12, cutoff 0.25 cycle per pixel). Attenuation correction was made numerically by assuming the object shape to be an ellipse for each slice and the attenuation coefficient to be uniform (0.1/cm). Correction for scatter photons was not performed. Image slices were set up parallel to the canthomeatal (CM) line and were obtained at 8-mm intervals through the entire brain. After SPECT measurements, CT scans were obtained with the same CM line as applied for SPECT in all subjects. All reconstructed images were transferred to a UNIX (Sun Microsystems, Palo Alto, CA) workstation for further analysis.

### Image Standardization

SPECT images were normalized globally by averaging the whole-brain radioactivity to 100 counts per pixel. After this normalization, all SPECT images were registered with respect to standard image to make target images similar in size and shape using linear and nonlinear parameters, taking the affine model as a starting point for normalization (11). Smoothing of the images was done using a Gaussian filter with an isotropic dimension of 10 mm. The mean SPECT HMPAO image of 18 normal subjects obtained in another study (13) in our department using a human brain atlas (14) was taken as a standard reference image.

### Validity of AIR for Alzheimer's Disease

SPECT images of the target subjects and the reference image were converted into binary images. The brain and nonbrain areas were assigned values of 1 and 0, respectively, with 40% of the maximum pixel value as the threshold. Reference and target images were added to calculate overlap area, with a value of 2, and nonoverlap areas, with values of 1. Inaccuracy index (IAI) was calculated as:

$$\text{IAI} = \frac{\text{nonoverlap area}}{\text{overlap area} + \text{nonoverlap area}} \times 100 (\%).$$

Using the same transformation matrix as for SPECT–SPECT registration, we spatially normalized respective CT scans and displayed them on a Talairach grid. Variance in size, maximum discrepancy in contours among target subjects (at three horizontal sections –10, 0 and +10 Talairach grid) and the medial and lateral openings of lateral sulci were noted in the X (side to side of brain) and Y (anteroposterior) planes on transverse slices. Diagonal distances for each point were calculated using the formula reported previously (15):

$$\text{diagonal distance} = \sqrt{\Delta x^2 + \Delta y^2},$$

where  $\Delta x$  and  $\Delta y$  = differences of standard and target images in X and Y planes, respectively.

### Comparison of Alzheimer's Disease and Controls

The standardized CBF images were used to calculate the mean images for patients and control subjects. Group comparison of patients versus controls was performed on a voxel-by-voxel basis using statistical parameter mapping (SPM96). The resulting set of voxel values for each contrast constitute a statistical parametric map of the t statistic SPM[t].

A brain atrophy index (BAI) was calculated for each subject using a computer program (16). After specifying the appropriate design matrix, we estimated the covariant effects (negative correla-

tion) of aging and atrophy on CBF according to the general linear model at each and every voxel.

The SPM[t] obtained in group comparison and in covariance analysis was transformed to SPM[z] with a threshold of 3.09 ( $P = 0.001$  uncorrected). The resulting foci were then characterized in terms of spatial extent ( $k$ ) and peak height ( $u$ ). The significance of each region was estimated using distributional approximation from the theory of Gaussian fields (17). This characterization is in terms of the probability that a region of the observed number of voxels could have occurred by chance [ $P(n_{\max} > k)$ ] or that the peak height observed could have occurred by chance [ $P(z_{\max} > u)$ ] over the entire volume analyzed (i.e., a corrected  $P$  value).

## RESULTS

The inaccuracy index for AIR calculated on CBF images (based on voxel data) was  $1.8\% \pm 0.11\%$  and  $2.3\% \pm 0.28\%$  for healthy subjects and AD patients, respectively. Anatomical variance noted on realigned structural images ranged from 4.6 to 4.9 mm for controls and AD patients, respectively. These values show that the inaccuracy in standardization procedure in terms of anatomical variance was far below the resolution of gamma camera, hence it was acceptable at least for SPECT data from currently available instruments. BAIs calculated by the computer program differed significantly between the two groups ( $P < 0.001$ ), the values being  $0.911 \pm 0.038$  and  $0.974 \pm 0.01$  for patients and controls, respectively.

Figure 1 shows mean rCBF images of patients and age-matched control subjects. Mean images of healthy subjects show relatively higher counts in parietal and frontal

regions. Figure 2 is a Z map (controls and patients) showing significant differences in CBF values in the frontal, parietal and temporal regions ( $P < 0.001$ ) [height threshold  $P(z_{\max} > u)$ , extent threshold  $P(n_{\max} > k)$ ]. Periventricular regions also show significant Z values, which is the effect of global normalization. Figures 3 and 4 show parametric maps correlating atrophy index and age of patients against voxel-based CBF values. Atrophy has a minimal effect on the blood flow of the intact cortical areas, whereas age has a significant effect on CBF.

## DISCUSSION

The AIR program can align and register brain images obtained with different modalities based on voxel data, thus allowing generation of a mean image from aligned brain images of sample subjects of a population. Validity of AIR for SPECT-SPECT transformations in AD has not been tested. We demonstrated the accuracy of AIR for mean image generation from the SPECT brain images after alignment and registration.

The observed inaccuracy from IAI was on average 2.3% or less; this indicates that transformation by AIR is fairly accurate and acceptable even in those cases with advanced age and atrophy. The previously reported accuracy of AIR for transformation of SPECT images of normal subjects using only linear parameters was 98%–99% (11). Contrary to that study in which the target population was relatively younger, this study included individuals with successful advanced aging (controls) and AD patients. Both groups had atrophy, but atrophy was more marked in the AD group

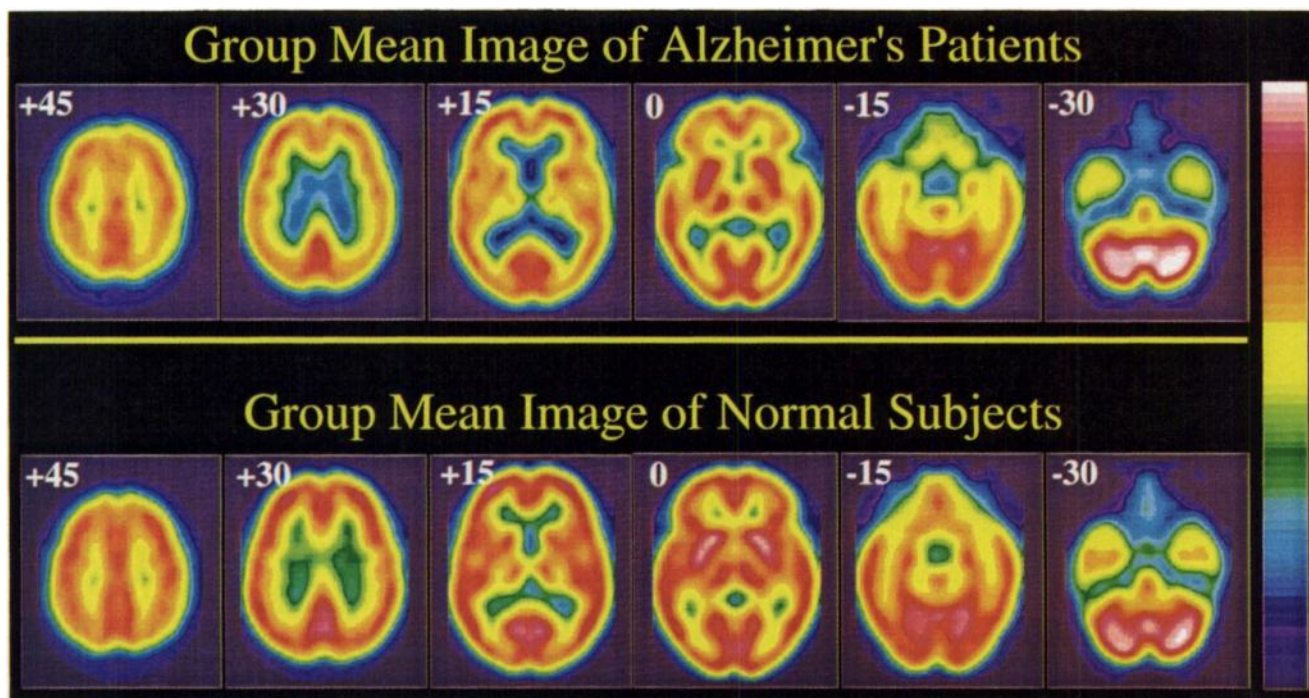


**FIGURE 1.** Group mean  $^{99m}\text{Tc}$ -HMPAO SPECT images of brain in patients with AD and healthy subjects. Mean global value is 100 counts per pixel. Horizontal slices are with reference to Talairach grid. Anterior is at top of image and subject's right is on left.

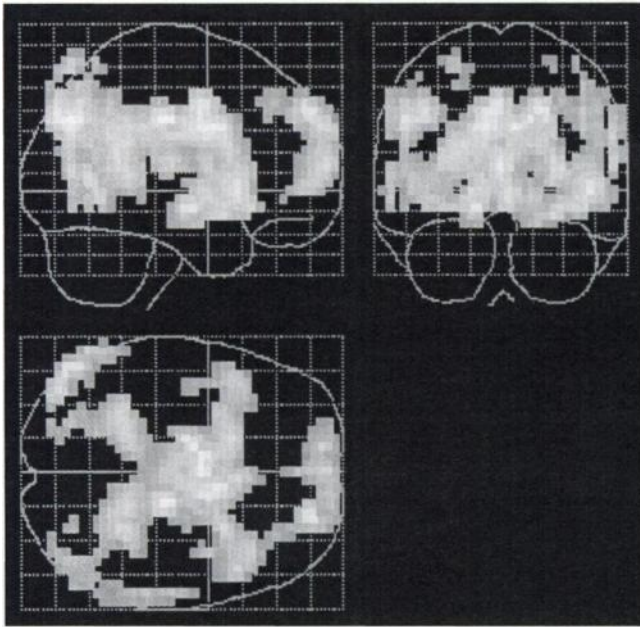


**FIGURE 2.** Z map (mean image of normal subjects and mean image of AD patients) displayed on glass brain. It shows statistically significant differences in frontal, parietal and temporal regions. Image in periventricular regions is due to effect of global normalization.

(mean values of atrophy indices 0.974 and 0.911, respectively). However, our careful use of nonlinear parameters of registration led to fairly accurate spatial normalization. Maximum error in terms of anatomical landmarks measured on CT scans was 4.9 mm, which is comparable with previous studies in which structural images were used for transformation and the SD of anatomical variance was

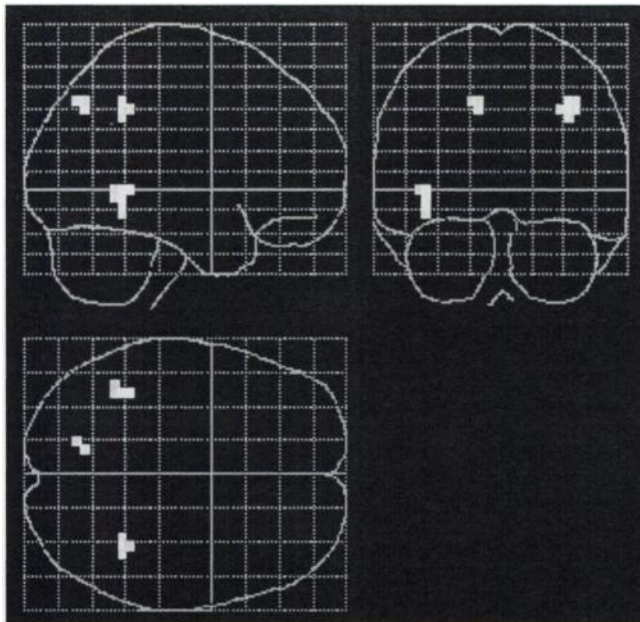


**FIGURE 3.** Statistical maps show correlation between atrophy (calculated on CT scans) and rCBF ( $^{99m}\text{Tc}$ -HMPAO) images of AD patients.

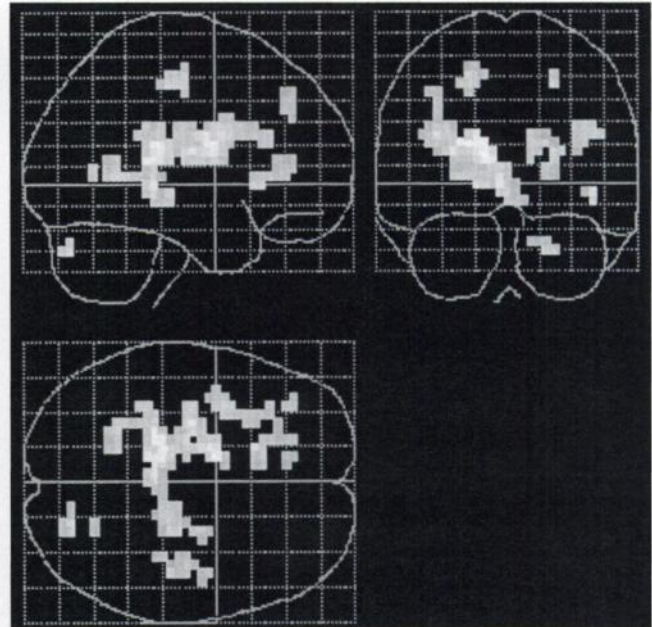


**FIGURE 4.** Statistical maps show correlation between age (in years at time of SPECT) and rCBF ( $^{99m}\text{Tc}$ -HMPAO) images of AD patients.

approximately 4.5 mm (14). When applying a transformation matrix of SPECT alignment to respective CT scans, there is always a propagation error in addition to errors in positioning and acquisition. However, the maximum error still proved to be below the resolution of the gamma camera (FWHM 8 mm) and can therefore be considered as within acceptable limits.

This prospective study was aimed at evaluating rCBF abnormalities in group mean images of AD patients; it revealed decreased blood flow in the frontal, parietal and temporal lobes whereas the primary cortical areas showed preserved CBF. Most of the previous studies showed parieto-temporal deficits as characteristic findings of AD (18–22). The finding of frontal lobe deficit revealed in this study might be the result of signal averaging and uniformity of population under study.

Changes in functional coupling between various regions of the brain leading to a decrease in CBF values could not be explained by simple geriatric change because, in this study, CBF images of patients were compared with those of controls. Moreover, covariance analysis has shown that mere age and atrophy cannot explain all the lower values of CBF in AD. Although advanced atrophy causes expansion in cerebrospinal fluid (CSF) space, it has minimal effect on blood flow of shrunken but intact cortical areas (at least at an early stage of AD). Atrophy-matched group comparison between normal and AD subjects (results not shown) confirmed this finding of covariance analysis. Aging has more impact on rCBF; however, even advanced age cannot explain all the findings. Voxel-based comparison between patients and controls must have canceled the effect of successful aging on CBF.

The relatively advanced atrophy observed in patients appears to be due to disease rather than to simple aging processes. We believe that comparison with age-matched normal subjects cancels out any atrophy related to successful aging, and the remaining part of atrophy is merely due to disease that needs to be evaluated with results. Local and global effects of atrophy on CBF images may be expected to disrupt the registration process. AIR assigns a zero value to CSF space (with the threshold setting used for registration). In this setup, the algorithm cannot differentiate between truly zero and atrophic areas. However, if one starts the registration with the affine model and forces the algorithm to go for unidirectional fit, this problem will be countered. Special options are available in AIR ( $-p10$ ,  $-p2$ , 0, etc.) to avoid untoward effects of missing data or misinterpretation of data. By this option, software derives registration parameters excluding the area affected by atrophy. Once the calculation of transformation matrix is over, it can be applied to whole-brain CBF data. Moreover, we have successfully registered rCBF images after the introduction of artificial cold defects (equal to 20 mL volume) with the help of AIR (23). Extrapolation of these results to the clinical environment suggests that advanced atrophy in patients does not yield or propagate any error during registration of SPECT rCBF images by AIR. Standard deviation of ratio images was used as cost function in the process of linear registration. This cost function has the advantage of being independent of image intensity, so registration will not be adversely affected in cases of advanced atrophy and age variance.

Although CBF image standardization and averaging facilitate pixel-by-pixel comparisons, theoretically error could arise from the original rCBF values if there is any missing data. Missing data in the reference image may lead to bizarre results during registration; however, the mean image, if used as the standard image, cannot have missing data. The standard brain image used in our study was the mean of HMPAO images for healthy volunteers with an average age of 51 y (range 34–63 y). The average age of the target subjects, in contrast, was around 70 y. However, both groups were treated equally, and standard deviation of ratio images was used as a cost function, so this effect may have been minimized, if not canceled out altogether.

We minimized interpolation artifacts during postreconstruction resampling by using sinc interpolation. The process of matrix calculation was stored in ASCII files. It was checked at the end of each step for any problem with registration process and positivity of Hessian matrix. When the Hessian matrix became nonpositive, we opted for special sampling and initialization of the ASCII file, which ultimately corrected the error. We also checked the results (images) at each stage of registration before inclusion in the final results.

On a Z map, significant values of the pixels were determined in two types of threshold—a critical height that a region had to reach and a critical size that a region must exceed to be considered significant. This step was taken to

avoid any risk of a wrong conclusion. The periventricular regions have shown up on a Z map, and this reflects the effect of global normalization (taking whole-brain activity as reference). As assessed in most clinical studies, we mainly considered changes in relative CBF.

Most studies assessing the accuracy of SPECT in AD have been retrospective with patient selection based on the diagnosis established at the time of scintigraphic evaluation. Prospective and consecutive studies, although difficult to perform because of the long follow-up, are more accurate guides for clinical practice (24). We therefore coupled our image analysis of consecutive cases with a clinical follow-up of sufficient duration to reduce diagnostic uncertainty. To confirm the diagnosis of AD, a follow-up of at least 1 y and reexamination by a psychiatrist were mandatory for the inclusion of SPECT CBF images in the analysis. As a result, the number of patients that could be definitely classified as AD was only 50% (13 out of 26) of the total patient population at the commencement. Because medication may effect CBF images through metabolic alterations (25–29), we performed our studies before starting any medication.

To our knowledge, this is the first prospective study aimed at the preparation of a mean image for AD patients after spatial normalization of individual images with the use of AIR. Effective comparison of group mean images of patients with that of age-matched normal subjects thereby proved possible, and the data generated in this prospective study should be useful as a reference for future projects.

This study showed that mere advanced atrophy and the effects of senility on CBF cannot explain all the deficits. Other factors should also be explored. Another innovative development might be the application of meso-HMPAO along with routine rCBF studies to image the antioxidant ability of the brain in normal controls and patients with AD. Longitudinal follow-up with the parallel glutathione imaging using meso-HMPAO may give new directions to research and clinical aspects of AD.

## CONCLUSION

AIR can transform SPECT images of AD patients with acceptable accuracy without the need for any corresponding structural image. Use of the standardization procedure enhances the confidence of characteristic findings. It also facilitates voxel-based comparisons allowing increased sensitivity and precision. AIR is operator independent, so multicenter and group studies can be easily performed.

The frontal regions of the brain, in addition to parietal and temporal lobes, may show reduced CBF in patients with AD even at an early stage.

The aging process has a more pronounced effect on CBF of intact cortical areas than that of atrophy, at least at an early stage of AD.

Covariance analysis showed that the reduced rCBF in parietal and frontal regions cannot be explained only by advanced atrophy and advanced aging process.

## ACKNOWLEDGMENTS

This study was supported in part by grants in aid for scientific research from the Ministry of Education, Science, Sports and Culture (09207102), JSPS-RFTF (97L00202), Telecommunication Advancement Organization and Ministry of Health and Welfare of Japan.

## REFERENCES

- Holman BL, Johnson KA, Gerada B, Carvalho PA, Satlin A. The scintigraphic appearance of Alzheimer's disease: a prospective study using Tc-99m HMPAO SPECT. *J Nucl Med.* 1992;33:181-185.
- Costa DC, Ell PJ, Burn A, Philpot M, Levy R. CBF tomograms with Tc-99m HMPAO in patients with dementia and Parkinson's disease. *J Cereb Blood Flow Metab.* 1988;8:S109-S115.
- Neary D, Snowden JS, North B, Goulding P. Dementia of frontal lobe type. *J Neurol Neurosurg Psychiatry.* 1988;51:353-361.
- Alpert N, Bradshaw J, Senda M, Correia J. The principal axis transformation: a method for image registration. *J Nucl Med.* 1989;30:776.
- Junck L, Moen JG, Hutchins GD, Brown MB, Kuhl DE. Correlation methods for centering, rotating, and alignment of functional brain images. *J Nucl Med.* 1990;31:1220-1226.
- Woods RP, Grafton ST, Holmes CJ, Cherry SR, Mazziotta JC. Automated image registration: I. General methods and intrasubject, intramodality validation. *J Comput Assist Tomogr.* 1998;22:141-154.
- Woods RP, Grafton ST, Watson JDG, Sicotte NL, Mazziotta JC. Automated image registration: II. Intersubject validation of linear and nonlinear models. *J Comput Assist Tomogr.* 1998;22:155-165.
- Woods RP, Mazziotta JC, Cherry SR. Automated image registration. In: Uemura K, et al., eds. *Quantification of Brain Function. Tracer Kinetics and Image Analysis in Brain PET.* Amsterdam, The Netherlands: Elsevier Science; 1993:391-398.
- Black KJ, Videen TO, Perlmutter JS. A metric for testing the accuracy of cross modality image registration: validation and application. *J Comput Assist Tomogr.* 1996;20:855-861.
- Imran MB, Kawashima R, Sato K, et al. Evaluation of accuracy in intersubject transformation of brain SPECT images using automated image registration (AIR). *Ann Nucl Med.* 1996;10(S):222.
- Imran MB, Kawashima R, Sato K, et al. Mean rCBF images of normal subjects using Tc-99m HMPAO by Automated Image Registration (AIR). *J Nucl Med.* 1998;32:203-207.
- Kimura K, Hashikawa K, Wtani H, et al. A new apparatus for brain imaging: four head rotating gamma single photon emission computed tomography. *J Nucl Med.* 1990;31:603-609.
- Koyama M, Kawashima R, Ito H, et al. Normal cerebral perfusion of Tc-99m HMPAO brain SPECT—evaluation by an anatomical standardization technique. *Jpn J Nucl Med.* 1995;32:967-977.
- Roland PE, Graufelds CJ, Wahlin J, et al. Human brain atlas: for high resolution functional and anatomical mapping. *Hum Brain Mapping.* 1994;1:173-184.
- Eberl S, Kanno I, Fulton RR, Ryan A, Hutton BF, Fulham MJ. Automated interstudy image registration technique for SPECT and PET. *J Nucl Med.* 1996;37:137-145.
- Takeda S, Matsuizawa T. Brain atrophy during aging: a quantitative study using computed tomography. *J Am Geriatr Soc.* 1984;32:520.
- Friston KJ, Frith CD, Liddle PE, Frachowiak RSJ. Comparing functional (PET) images. The assessment of significant change. *J Cereb Blood Flow Metab.* 1992;11:690-699.
- Haxby JV, Grady CL, Koss E, et al: Heterogeneous anterior posterior metabolic patterns in Alzheimer's type dementia. *Neurology.* 1988;38:1853-1863.
- Bensen DF, Kuhl DE, Hawkins RA, Phelps ME, Cummings JL, Tsai SY. The fluorodeoxyglucose <sup>18</sup>F scan in Alzheimer's disease and multi infarct dementia. *Arch Neurol.* 1983;40:711-714.
- Metter EJ, Riege WH, Kameyama M, Kuhl DE, Phelps ME. Cerebral metabolic relationships for selected brain regions in Alzheimer's, Huntington's and Parkinson's diseases. *J Cereb Blood Flow Metab.* 1984;4:500-506.
- Freidland RP, Budinger TF, Ganz E, et al. Regional cerebral metabolic alteration in dementia of the Alzheimer type: positron emission tomography with <sup>18</sup>F fluoro deoxyglucose. *J Comput Assist Tomogr.* 1983;7:590-598.
- Duara R, Grady CL, Haxby JV, et al. Positron emission tomography in Alzheimer's disease. *Neurology.* 1986;36:879-887.
- Kinomura S, Kawashima R, Sato K, Kinomura S, Imran MB, Fukuda H. Intersubject transformation of brain SPECT by automated image registration (AIR). Effects of defects in the target image. *Ann Nucl Med.* 1996;10(suppl):S222.
- Launes J, Sulkara R, Erkijuntti T, et al. Tc-99m HMPAO SPECT in suspected dementia. *Nucl Med Commun.* 1991;12:757-765.
- Kobari M, Fukuuchi Y, Shinohara T, Obara K, Nogawa S. Levodopa induced local cerebral blood flow changes in Parkinson's disease and related disorders. *J Neurol Sci.* 1995;128:212-218.
- Asanuma M, Hirata H, Kondo Y, Ogawa N. A case of progressive supranuclear palsy showing marked improvements of frontal hypoperfusion, as well as Parkinsonism with amitriptyline. *Rinsho Shinkeigaku.* 1993;33:317-321.
- Heiss WD, Hebold H, Klinkhammer P. Effect of piracetam on cerebral glucose metabolism in Alzheimer's disease as measured by positron emission tomography. *J Cereb Blood Flow Metab.* 1988;8:613-617.
- Geaney DP, Soer N, Shepstone BJ, Cowen PJ. Effect of central cholinergic stimulation on regional cerebral blood flow in Alzheimer disease. *Lancet.* 1990;335:1484-1487.
- Harkins SW, Taylor JR, Mattay US. Response to tacrine in patients with dementia to Alzheimer's type: cerebral perfusion change related to change in mental status. *Int J Neurosci.* 1996;84:149-156.